Supporting Information for: Controlling the Intermediate Structure of an Ionic Liquid for f-Block Element Separations

Carter W. Abney,†* Changwoo Do,‡ Huimin Luo,† Joshua Wright, §‖ Lilin He,‡ Sheng Dai†¶

† Oak Ridge National Laboratory, One Bethel Valley Road, P.O. Box 2008, Oak Ridge, TN 37831, U.S.A.

‡ Biology and Soft Matter Division, Neutron Sciences Directorate, Oak Ridge National Laboratory, P.O. Box 2008, Oak Ridge, TN 37831, U.S.A.

§ Advanced Photon Source, Argonne National Laboratory, 9700 Cass Ave, Lemont, IL 60439, U.S.A.

‖ Illinois Institute of Technology, 3300 S. Federal St, Chicago, IL, 60616, U.S.A.

¶ Department of Chemistry, University of Tennessee, Knoxville, TN 37966, U.S.A.

Table of Contents:

1. General Experimental

All chemicals and solvents were reagent grade and were used without further purification. Trihexyltetradecylphosphonium bromide ($[P_{666(14)}]Br$) was purchased from Aldrich, while HDEHP was purchased from Alfa Aesar. $[C_4mim][NTf_2]$ and $[P_{666(14)}][DEHP]$ were prepared as reported previously.[1-2] Water content was determined using an AQUAPAL III Karl-Fisher titrater. TALSPEAK simulant was prepared by dissolving $Lu(NO_3)_3$ of varying concentrations in an aqueous 0.1 M glycolic acid solution with 0.01 M diethylenetriamine-N,N,N',N'',N''-pentaacetic acid (DTPA), affording a solution with pH 3.24. Samples for SANS and XAFS investigations were prepared by contacting 1 mL of 0.4 M $[P_{666(14)}][DEHP]$ in $[C_4mim][NTf_2]$ with 1 mL TALSPEAK simulant for 60 minutes in a vibrating mixer. The samples were then centrifuged at an RCF of 11300 g for 5 minutes and the aqueous phase removed.

2. SANS Data Collection and Processing

SANS data were collected on Beamline-6, EQ-SANS, at the Spallation Neutron Source of Oak Ridge National Laboratory.[3] IL samples were transferred to quartz Helma cells possessing path lengths of 1 mm, then sealed with Teflon caps fastened with Parafilm. Data were collected at room temperature, with detectors located at 8 m, 4 m, and 1.3 m from the sample, corresponding to low, medium, and high q-range. The instrument was used in 60 Hz mode with minimum wavelengths of 10, 6, 1.5 Å, for 8m, 4m, and 1.3m detector locations respectively, to provide an effective q-range of ~ 0.003 Å^{-1} to 1.5 Å^{-1} Data were reduced and processed using MantidPlot using standard procedures to correct for detector sensitivity, instrument dark current, sample transmission and empty cell background.[4] Data fitting was performed using SasView 3.1.2 software (http://www.sasview.org).

3. XAFS Data Collection and Processing

XAFS data were collected on beamline 10-ID-B at the Advanced Photon Source of Argonne National Laboratory.[5] ILs contacted with 0.025 M and 0.010 M $Lu(NO_3)_3$ in TALSPEAK simulant were sealed in a polyethylene sample vials, with spectra collected at the Lu L_{III}-edge (9244 eV) at ambient temperature and pressure. Data were collected using a Lytle-type fluorescence detector. The x-ray white beam was monochromatized by a Si(111) monochromater with higher-order harmonics removed through use of a Rh harmonic rejection mirror. Due to the high flux and configuration of the beamline, the x-ray energy was varied at a constant rate across the absorption edge; neither step size nor dwell time changed as a function of energy; 200 scans were collected for each sample.

Data were processed and fit using the Athena and Artemis programs of the IFEFFIT package based on FEFF 6.[6-7] Upon importing, data were rebinned with grids of 10 eV, 0.5 eV, and 0.005 $Å^{-1}$ for the pre-edge region, near-edge region, and EXAFS region, respectively. Spectra were averaged in $\mu(E)$ prior to normalization. The background was removed and the data were assigned an Rbkg value of 1.0 prior to normalizing to obtain a unit edge step. Data were fit with k^3-weighting, appropriate for a heavy absorbing element surrounded by light scatterers. The first shell of atoms coordinating the Lu absorber was determined using an Lu-O single scattering path at 2.20 Å. The amplitude reduction factor was set to 1, while fitted variables included the degeneracy of the scattering path (N_{degen}), the change in the effective half-path length of the Lu-O scatterer (ΔR), the relative mean squared displacement of the scatterer (σ^2), and the energy shift of the photoelectron (ΔE_0). For each fit, the number of variables was not permitted to exceed 2/3 the number of independent points, complying with the Nyquist criterion.[8]

4. Derivation of Eq. 1

f = Volume Fraction of Extracted Water

$\rho_{structure}$ = Scattering Length Density of Ionic Liquid Microstructural Feature

ρ_{water} = Scattering Length Density of generic water

ρ_{H2O} = Specific Scattering Length Density of H_2O (-0.56×10^{-6} Å^{-2})

ρ_{D2O} = Specific Scattering Length Density of D_2O (6.39×10^{-6} Å^{-2})

$\rho_{(IL)}$ = Scattering Length Density of IL in Microstructure ($0.5 \times \rho_{(C4mim)} + 0.5 \times \rho_{(DEHP)} = 0.67 \times 10^{-6}$ Å^{-2})

The $\rho_{structure}$ is equal to the ρ of the water in the structure plus the ρ of the IL in the structure, weighted by their corresponding volume fractions. With f defined as the volume fraction of extracted water, the remainder of the structure must be the IL.

$$\rho_{structure} = [f \times \rho_{water}] + [\rho_{(IL)} \times (1\text{-}f)] \tag{S1}$$

The value of $\rho_{structure}$ can be defined by Eq. S1 for H_2O and D_2O, as provided in Eqs. S2 and S3, respectively.

$$\rho_{structure(H2O)} = [f \times \rho_{H2O}] + [\rho_{(IL)} \times (1\text{-}f)] \tag{S2}$$

$$\rho_{structure(D2O)} = [f \times \rho_{D2O}] + [\rho_{(IL)} \times (1\text{-}f)] \tag{S3}$$

Eq. S2 can be rearranged to afford an equation for f, provided in Eq. S4.

$$\rho_{structure(H2O)} = f \times \rho_{H2O} + \rho_{(IL)} - f \times \rho_{(IL)}$$

$$\rho_{structure(H2O)} = f\,(\rho_{H2O} - \rho_{(IL)}) + \rho_{(IL)}$$

$$f = \frac{\rho_{structure(H2O)} - \rho_{(IL)}}{\rho_{H2O} - \rho_{(IL)}} \tag{S4}$$

Having defined f as a function of $\rho_{structure(H2O)}$, we substitute Eq. S4 into Eq. S3 to obtain Eq. 1 in the text, which relates $\rho_{structure(H2O)}$ to $\rho_{structure(D2O)}$ and allows simultaneous refinement of these values through data fitting.

$$\rho_{Structure\,(D2O)} = \frac{\rho_{structure(H2O)} - \rho_{(IL)}}{\rho_{H2O} - \rho_{(IL)}} \times (\rho_{D2O} - \rho_{(IL)}) + \rho_{(IL)} \tag{1}$$

5. Supplementary Data and Figures
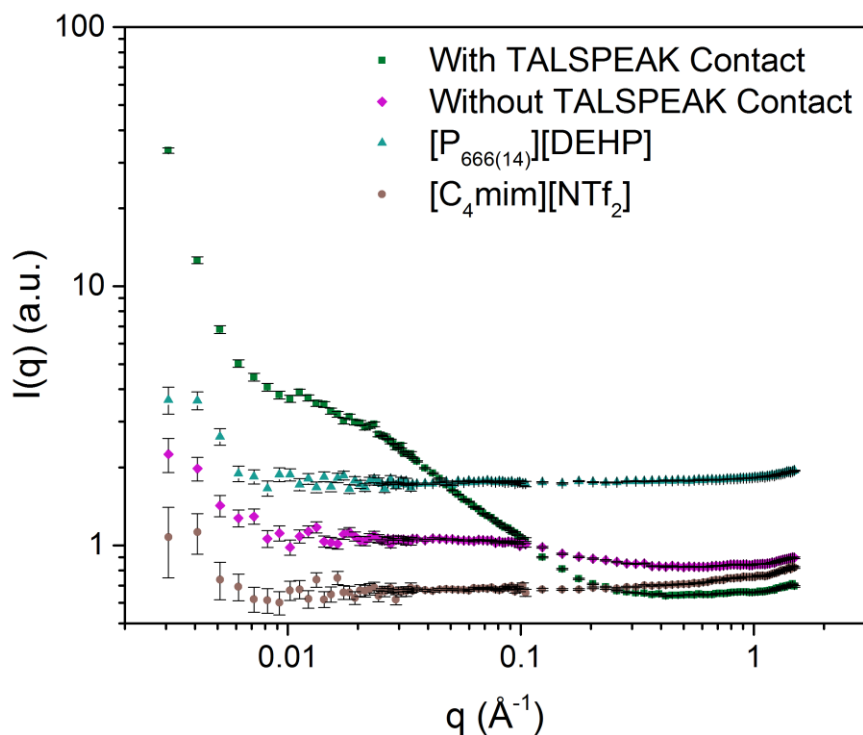
Figure S1. SANS data for $[P_{666(14)}][DEHP]$ in $[C_4mim][NTf_2]$ prior to contact with TALSPEAK simulant (grey diamonds), as well as the individual constituent ionic liquids, $[P_{666(14)}][DEHP]$ (blue triangles) and $[C_4mim][NTf_2]$ (brown circles). The data for $[P_{666(14)}][DEHP]$ in $[C_4mim][NTf_2]$ contacted with TALSPEAK containing 0.0025 M $Lu(NO_3)_3$ (as plotted in Figure 1) are displayed as green squares for comparison. Data have not been artificially offset.

Table S1. Solid Cylinder Fit of SANS Data from Contact of $[P_{666(14)}][DEHP]$ / $[C_4mim][NTf_2]$ with TALSPEAK Simulant with 0.0025 M $Lu(NO_3)_3$

Length (Å)	Radius (Å)	Scale	χ_v^2	R_g (Å)
171 ± 2	11.66 ± 0.07	0.049 ± 0.001	3.5	50

Table S2. Calculated Scattering Length Densities for Ionic Liquid Constituents

Component	Molecular Formula	Molar Weight (g mol^{-1})	Density (g mL^{-1})	Scattering Length Density ($\times 10^{-6}$ Å^{-2})
Water	H_2O	18.0	1.00	-0.56
$[P_{666(14)}]^+$	$PC_{32}H_{68}$	483.4	0.96	-0.44
$[DEHP]^-$	$PO_4C_8H_{18}$	209.1	0.96	0.39
$[C_4mim]^+$	$N_2C_8H_{15}$	139.1	1.39	0.95
$[NTf_2]^-$	$NS_2O_4C_2F_6$	280.1	1.39	2.56
Water-d	D_2O	20.0	1.11	6.39

Table S3 Refined Fit Parameters for Simultaneous Fit of Protiated and Deuterated Data Sets with Solid Cylinder Model

Variable	H_2O	D_2O
Background (cm^{-1})	0.6617 ± 0.0002	0.6654 ± 0.0002
Length (Å)	217 ± 2	54.0 ± 0.4
Radius (Å)	11.98 ± 0.06	
Scale	$3.63 \times 10^{-13} \pm 3 \times 10^{-15}$	
$\rho_{cylinder}$ (Å^{-2})	0.639 ± 0.002	0.816 ± 0.002
$\rho_{solvent}$ (Å^{-2})	1.7 (fixed)	

Table S4. Comparison of Fitted SANS Data from Contact of $[P_{nnn(14)}][DEHP]$ / $[C_4mim][NTf_2]$ ($n = 4, 6$) with TALSPEAK Simulant Containing 0.0025 M Lu(NO$_3$)$_3$

Sample	Length (Å)	Radius (Å)	Scale	χ_v^2	R_g (Å)
$n = 6$	171 ± 2	11.66 ± 0.07	0.049 ± 0.001	3.5	50
$n = 4$[a.]	21.9 ± 0.5	9.2 ± 0.2	0.059 ± 0.002	1.2	11

a. Fit using ellipsoidal form factor. The length column refers to the radius a, oriented along the rotation axis of the ellipsoid, while the radius column refers to radii b and c, oriented perpendicular to the rotation axis of the ellipsoid.

Table S5. Fit of SANS Data from Contact of $[P_{666(14)}][DEHP]$ / $[C_4mim][NTf_2]$ with TALSPEAK Simulant Containing Different Lu(NO$_3$)$_3$ Concentrations

Sample	Length (Å)	Radius (Å)	Scale	χ_v^2	R_g (Å)
0.0025 M	171 ± 2	11.66 ± 0.07	0.049 ± 0.001	3.5	50
0.025 M	165 (Fixed)[a.]	11.10 ± 0.07	0.051 ± 0.001	8.9	49
0 M	166 ± 2	11.40 ± 0.07	0.050 ± 0.001	4.0	49

a. The length of the ellipsoid was fixed, to be consistent with values obtained for other samples. Allowing this parameter to vary freely resulted in a fit which was equally good statistically, but afforded physically questionable values, such as an unreasonably small radius.

Table S6. Fit Parameters for EXAFS data of Ionic Liquids Following Contact with TALSEPAK simulant.

	0.01 M $Lu(NO_3)_3$	0.025 M $Lu(NO_3)_3$
Coord. No.	9.5 ± 2.4	9.2 ± 2.4
Δ E_0	7.3 ± 2.2	7.8 ± 2.2
R (Å)	2.24 ± 0.04	2.24 ± 0.02
σ^2 (× 10^{-3} Å^2)	9 ± 4	9 ± 4

Table S7. Water content as a function of metal concentration for $[P_{666(14)}][DEHP]$ in $[C_4mim][NTf_2]$ as determined by Karl-Fisher titration

Sample	Water concentration (ppm)
Before contact	4506
No $Lu(NO_3)_3$	6489
0.0025 M $Lu(NO_3)_3$	10608
0.025 M $Lu(NO_3)_3$	14883

6. References

(1)   Sun, X. Q.; Luo, H. M.; Dai, S. Solvent Extraction of Rare-Earth Ions Based on Functionalized Ionic Liquids. *Talanta* **2012,** *90*, 132-137.

(2)   Luo, H. M.; Dai, S.; Bonnesen, P. V. Solvent Extraction of Sr^{2+} and Cs^+ Based on Room-Temperature Ionic Liquids Containing Monoaza-Substituted Crown Ethers. *Anal. Chem.* **2004,** *76*, 2773-2779.

(3)   Zhao, J. K.; Gao, C. Y.; Liu, D. The Extended Q-range Small-Angle Neutron Scattering Diffractometer at the SNS. *J. Appl. Crystallogr.* **2010,** *43*, 1068-1077.

(4)   Arnold, O.; Bilheux, J. C.; Borreguero, J. M.; Buts, A.; Campbell, S. I.; Chapon, L.; Doucet, M.; Draper, N.; Ferraz Leal, R.; Gigg, M. A.; Lynch, V. E.; Markvardsen, A.; Mikkelson, D. J.; Mikkelson, R. L.; Miller, R.; Palmen, K.; Parker, P.; Passos, G.; Perring, T. G.; Peterson, P. F.; Ren, S.; Reuter, M. A.; Savici, A. T.; Taylor, J. W.; Taylor, R. J.; Tolchenov, R.; Zhou, W.; Zikovsky, J. Mantid—Data Analysis and Visualization Package for Neutron Scattering and SR Experiments. *Nucl. Instrum. Methods Phys. Res., Sect. A* **2014,** *764*, 156-166.

(5)   Segre, C. U.; Leyarovska, N. E.; Chapman, L. D.; Lavender, W. M.; Plag, P. W.; King, A. S.; Kropf, A. J.; Bunker, B. A.; Kemner, K. M.; Dutta, P.; Duran, R. S.; Kaduk, J. In *The MRCAT Insertion Device Beamline at the Advanced Photon Source*, Synchrotron Radiation Instrumentation: Eleventh U.S. National Conference, New York, NY (USA), Pianetta, P., Ed. American Institute of Physics: New York, NY (USA), 2000; pp 419-422.

(6)   Ravel, B.; Newville, M. Athena, Artemis, Hephaestus: Data Analysis for X-ray Absorption Spectroscopy using IFEFFIT. *J. Synchrotron Radiat.* **2005,** *12*, 537-541.

(7)   Rehr, J. J.; Albers, R. C. Theoretical Approaches to X-ray Absorption Fine Structure. *Rev. Mod. Phys.* **2000,** *72*, 621-654.

(8)   Calvin, S. *XAFS for Everyone*. CRC Press: Boca Raton, FL, 2013.